Check for updates

Received: 4 August 2021 | Revised: 26 November 2021 | Accepted: 28 December 2021

DOI: 10.1002/rcs.2360

ORIGINAL ARTICLE

The International Journal of Medical Robotics and Computer Assisted Surgery

WILEY

A novel arthroscopic pre-curved cannula with both flexibility and high stiffness

Chulmin Park[1,2] | Jeongryul Kim[2] | Yonghwan Moon[3,4] | Keri Kim[3,5]

[1]Medical Device Development Center, Daegu-Gyeongbuk Medical Innovation Foundation, Daegu, Republic of Korea

[2]Robotics & Media Institute, Korea Institute of Science and Technology (KIST), Seoul, Republic of Korea

[3]Augmented Safety System with Intelligence Sensing and Tracking (ASSIST), Korea Institute of Science and Technology, Seoul, Republic of Korea

[4]School of Mechanical Engineering, Korea University, Seoul, Republic of Korea

[5]Division of Bio-Medical Science and Technology, University of Science and Technology, Daejeon, Republic of Korea

Correspondence

Keri Kim, Augmented Safety System with Intelligence Sensing and Tracking (ASSIST), Korea Institute of Science and Technology, 5 Hwarang-ro 14-gil, Sungbuk-gu, Seoul 02792, Republic of Korea.
Email: jazzpian@kist.re.kr

Jeongryul Kim, Robotics and Media Research Institute, Korea Institute of Science and Technology (KIST), 5 Hwarang-ro 14-gil, Sungbuk-gu, Seoul 02792, Republic of Korea.
Email: namsookim86@gmail.com

Funding information

National Research Council of Science and Technology, Grant/Award Number: CRC-20-02-KIST

Abstract

Background: Curved surgical instruments are being developed to expand the workspace of straight surgical instruments. They are required to have a small diameter and high stiffness.

Methods: We developed a double-spring pre-curved cannula (DSPC) for electrocauterization, which has curved movements controlled solely by translational motion, and high stiffness via wire tension. It comprises a straight extension spring, pre-curved flat spring and braided high-modulus polyethylene line. A handheld device was designed for intuitive DSPC manipulation. The cannula has a 3.9 mm diameter and serves as a protective tube such that the electrode can safely reach the lesion.

Results: Experimental results demonstrate that the DSPC has ideal curvature and maximum stiffness of 1.38 N/mm. In a cadaveric study, the DSPC reached the inferior glenohumeral ligament, which conventional surgical instruments cannot access, and surgeons successfully performed electrocauterization.

Conclusions: The designed DSPC is effective for future use in forceps, curettes and surgical robots.

KEYWORDS

cadaveric study, high stiffness, minimally invasive surgery, pre-curved mechanism, spring-wire mechanism, variable stiffness

1 | INTRODUCTION

There is growing interest in minimally invasive surgeries (MISs), which are preferred by many patients because they leave few scars and allow rapid recovery. Arthroscopic surgery (AS), one of the various types of MISs, is being performed widely for the treatment of joint diseases such as those affecting the shoulders, hips, and knees.[1–3] An AS is conducted by making several 5-mm holes in the skin around a patient's joints and then inserting an arthroscope and surgical instruments such as electrocautery tools, forceps and curettes.[4,5] Images of these instruments can be transmitted through the arthroscope and seen on a display, so that the surgeon can operate the instruments appropriately to treat the lesion.

Many surgical instruments related to AS have been developed. The diameter of these instruments is decreasing to reduce the required size of the hole in the patient's skin, and they are now being developed to provide a relatively large workspace within narrow intra-articular spaces.[6] In addition, as mentioned above, although the surgical instruments used in AS are utilized for diverse purposes, a common issue is that many require a high stiffness.[7] For example,

 © 2022 John Wiley & Sons Ltd.

electrocautery devices should be able to apply pressure and scrape the tissue to burn lesions, forceps should be able to lift or tear tissue, and curettes should be able to scrape tissue and bone. Having a high stiffness can provide surgeons with better controllability and higher surgical success rates. Therefore, future surgical instruments must have the following characteristics: (1) high stiffness, (2) small diameter and (3) large workspace.

In general, most surgical instruments used in hospitals for AS are straight or curved with no change in tip flexion. If the position of a lesion is deep and narrow within the human body, it is difficult for the existing rigid instruments to approach the target.[8] Furthermore, even if they can reach it, tissues and bones around the joints may be damaged.[9] In addition, there is a case for making new portals to easily access the lesion,[10] but critical nerves passing around the joints may be injured in the process.[9,11] Thus, owing to the complexity and length of the surgery, the surgeons can become very fatigued.

To solve the above problems, handheld devices with a bendable tip[12] and manipulators with multiple degrees of freedom[13–18] have been developed. Surgical instruments for AS should be 5 mm or less in diameter because the procedure is performed through the portal, and they should have curved wrist joints rather than pin wrist joints because the bones around the joint are usually round. If manipulators such as serial joints, which make up most of the curved wrist type, have multiple degrees of freedom, the diameter and size of the driving parts increase, and it becomes heavy because the number of wires and motors increases. Therefore, it is not suitable for use as a handheld device. Even though the diameter and size of the driving parts can be reduced by minimizing the required degrees of freedom, the type of surgical tasks that can be performed is limited because the stiffness and payload become relatively low.

A pre-curved tip is a typical mechanism used to achieve a large workspace with a relatively small diameter and degree of freedom. RotaTip® is a commercially available product that operates with a similar mechanism.[19] However, it has a diameter of 5 mm and is bent at the shaft, not the tip of the device. In addition to this product, the pre-curved mechanism has been studied using Nitinol (Ni–Ti), a superelastic material. Cuschieri developed a variable-curvature spatula with Ni–Ti,[20] and Okazawa et al. designed a handheld steerable pre-curved needle device with Ni–Ti.[21] Webster III et al. developed a snake-like surgical robot for use as an active cannula that overlaps several pre-curved Ni–Ti tubes.[22,23] Related studies have shown that the pre-curved tips are made of Ni–Ti and are generally used for needles. Although a snake-like robot was developed for cannula, it is difficult to reduce the radius of curvature and have a high stiffness owing to the material properties of Ni–Ti. Many studies have been conducted to develop a mechanism for changing the stiffness of the manipulators of surgical robots. Kim et al. developed a stiffness-adjustable hyper redundant manipulator with multiple rolling joints and used a variable neutral-line mechanism.[24] In addition, some research groups used a layer jamming mechanism,[25] a granular jamming mechanism,[26,27] active heating and cooling mechanisms,[28] and shape memory alloy-based sheath structure[29] to control the stiffness. However, these mechanisms have a diameter of more than 15 mm and the volume of the drive unit is large; therefore, the types of surgery in which they can be used are limited.

In this study, we developed a novel pre-curved cannula that has high stiffness and, with a 5 mm diameter, is smaller than general arthroscopic instruments. It is designed for capsular release surgery, and we describe the design of the cannula, as well as the structure of the handheld device in this paper. After the device was completed, we performed a position accuracy test according to the advancing and stiffness tests. We then compared the results of the stiffness test with the contact force that occurs when surgeons use existing electrocautery devices. Finally, we evaluated the performance of the cannula device in a cadaveric study.

2 | MATERIALS AND METHODS

We have developed a double-spring pre-curved cannula (DSPC) with a small diameter, high stiffness and large workspace compared to conventional surgical instruments. As shown in Figure 1A, the DSPC consists of an extension spring, a flat spring and a braided line (polyethylene line) with high-modulus polyethylene. The extension spring is straight and functions as a surgical instrument channel. The flat spring is pre-curved and functions to maintain a bent shape even though it is integrated into the extension spring by welding. This is possible because the flat spring has a higher stiffness than the extension spring. The proximal part of the extension spring is connected to an inner tube with the same outer diameter, and the inner tube is a straight and rigid structure. The welded areas are between the extension spring and the flat spring, between the extension spring and the inner tube, and between the extension spring and the inner tube. More specifically, the three parts become one part through welding, and when the inner tube has translational movement, the extension spring and the flat spring move together. Because the outer tube is fixed, the DSPC is inserted into the straight outer tube and comes out from it according to the translational movement of the inner tube. The PE line (Sufix 832, Rapala) is fixed below the tip of the extension spring and functions to control the stiffness through tension. This section describes the process by which the DSPC was designed for capsular release surgery and the structure of a handheld device that uses the DSPC. When the DSPC enters the outer tube, as shown in Figure 1B, it stretches to fit into the straight outer tube. However, when the DSPC comes out of the outer tube, its shape is restored to its previous curved state.

2.1 | Extension spring

The extension spring is designed according to the shape of the humeral head, and the reference shape is shown in Figure 2. Because the average diameter of the humeral head is 49.0 mm,[30] the inner radius of curvature of the extension spring is r_i = 24.5 mm when it is bent 90° to reach under the humeral head. As shown in Figure 3, the

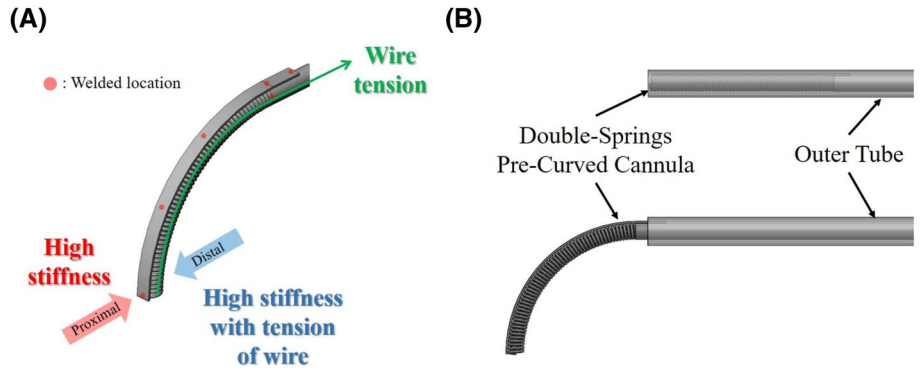

FIGURE 1 Design of the double-spring pre-curved cannula (DSPC). The DSPC consists of an extension spring, a flat spring and a braided line with high-modulus polyethylene. (A) The DSPC is welded at the six red dots. This creates a high stiffness in the proximal direction and a low stiffness in the distal direction. However, wire tension also creates a high stiffness in the distal direction. (B) The DSPC enters (upper image) and comes out of (lower image) a straight outer tube

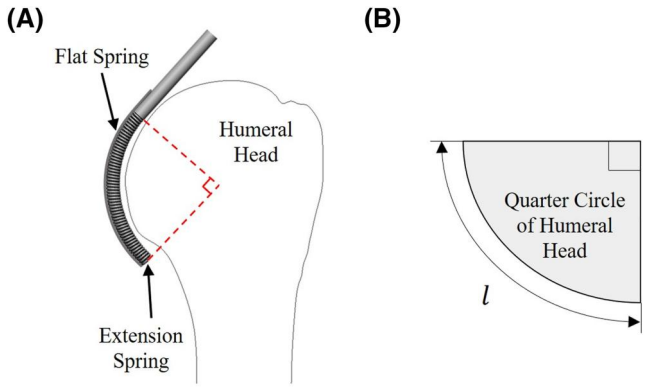

FIGURE 2 (A) Design of the double-spring pre-curved cannula according to the shape and size of the humeral head. (B) Arc length indication of the quarter humeral head

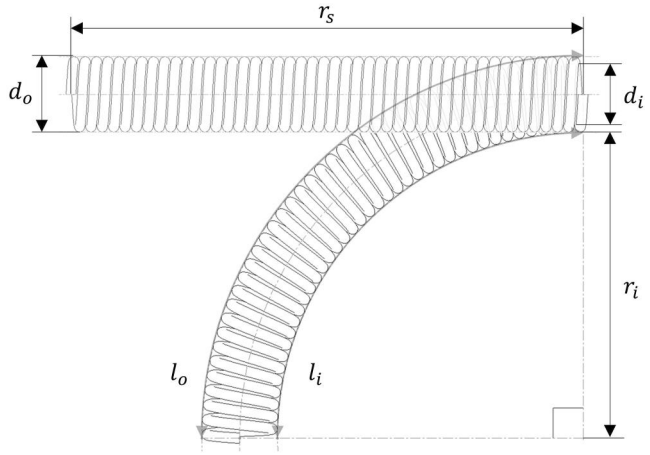

FIGURE 3 Size indication of the extension spring: straight and bent at 90°. The original shape is straight, and the curved shape results from integration with a pre-curved flat spring

length of the inner arc of the curved extension spring l_i and the arc length of the quarter circle l based on the diameter of the humeral head can be expressed as follows:

$$l_i = l = \frac{\pi r_i}{2} \tag{1}$$

From Equation (1), l_i = 38.5 mm, and the length of the linear extension spring r_s is equal to l_i because the pitch of the inner arc is 0 mm when it is bent at 90°. The inner diameter of the extension spring d_i was determined to be 1.7 mm considering not only that the electrode diameters[31] for the DSPC and the PE line were 1.1 and 0.28 mm, respectively, but the PE line was also knotted at the end of the extension spring. The outer diameter of the extension spring d_o was set to 2.5 mm considering laser welding with a flat spring and the thickness of the extension spring: r_s = 38.5 mm, d_o = 2.5 mm and d_i = 1.7 mm.

2.2 | Flat spring

The flat spring has a quarter-circle shape, as shown in Figure 4, unlike the linear extension spring because it is the main part that makes the cannula pre-curved. The flat spring is easier to manufacture in a bent shape compared to the extension spring. And since the flat spring has high stiffness, its shape does not change when combined with the straight extension spring. As the flat spring is located in the upper part of the extension spring, the length of the outer arc of the extension spring l_o is equal to the inner arc length of the flat spring L_i:

$$L_i = l_o = (r_i + d_o)\frac{\pi}{2} \tag{2}$$

Because $l_o = L_i$ = 42.4 mm, the inner radius of the flat spring R_i is 27.0 mm. Therefore, the central axis radius of the flat spring R_n is expressed as follows:

$$R_n = R_i + \frac{h}{2} \tag{3}$$

where h is the thickness of the flat spring.

From Equation (3), $R_n > R_i$ = 27.0 mm, and h must be known to obtain the correct value of R_n. As shown in Figure 4, h can be derived from the deflection (δ_y) and the maximum stress (σ_{max}) of the flat

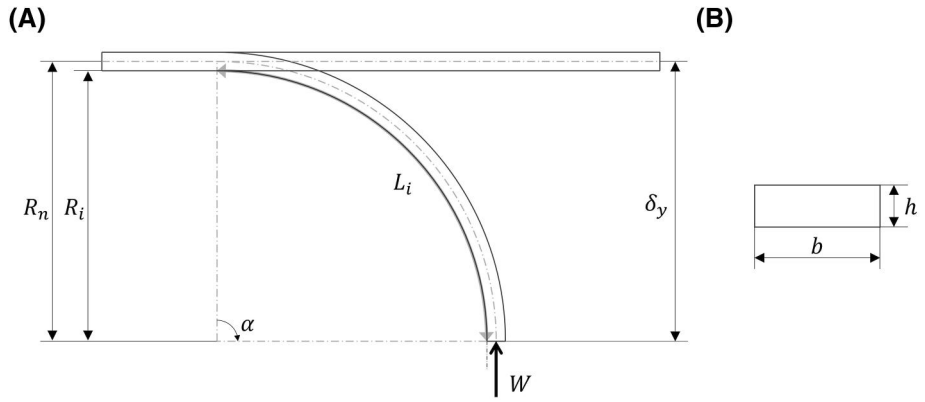

FIGURE 4 (A) Size indication of the flat spring: straight and bent at 90°. The original shape is straight, and the curved shape develops after the force W is applied. (B) Size indication in sectional view of the flat spring

spring when a force W acts on its tip with a central angle α. δ_y and σ_{max} are expressed as follows:

$$\delta_y = \frac{12WR_n^3}{bh^3E}(0.5\alpha - 0.25 \sin 2\alpha) \quad (4)$$

$$\sigma_{max} = \frac{6WR_n \sin \alpha}{bh^2} \quad (5)$$

where b and E are the width of the flat spring and the elastic modulus (186 GPa), respectively, and $\alpha = \frac{\pi}{2}$.

When the pre-curved flat spring exits the interior of the outer tube, plastic deformation should not occur because the original shape and angle must be maintained. The yield point of stainless steel, σ_{max}, should be less than 880 MPa. Furthermore, as shown in Figure 4, the deflection of the flat spring applicable to the DSPC, δ_y can be obtained from the difference between the arc length and radius of the flat spring, taking into account the insertion inside the straight outer tube:

$$\delta_y \geq R_n \quad (6)$$

Equations (4)–(6) were used to determine the thickness h and width b of the flat spring. We calculated the optimal values of h and b for a force W acting on the end of the flat spring by setting h in the range 0.16–0.45 mm in 0.01 mm increments and b in the range 0.6–3.5 mm in 0.1 mm increments. W was selected as the maximum value that satisfies Equations (5) and (6), decreasing from 10 to 0.001 N. The results are shown in Figure 5. This shows the deflection and stress of the flat spring according to h and b, and it can be confirmed that all the values of the deflection graph are within the yield point. In addition, the deflection graph confirms that the deflection greatly changes according to h rather than b. In the deflection graph, a plane across a curved graph is R_n, which is the right side of Equation (6), and values above the plane are candidate values of δ_y. Considering the durability and stiffness of the flat spring, the h nearest to the R_n was selected, and the value was 0.2 mm. Therefore, it was confirmed that R_n = 27.1 mm. b was set to 1.7 mm, which is equal to the inner diameter of the extension spring in consideration of the protruding part of the flat spring when the two springs were combined: h = 0.2 mm, b = 1.7 mm, R_n = 27.1 mm. W is a value corresponding to the values of h and b when F = 0.386 N.

2.3 | Double-springs pre-curved cannula and handheld device

As shown in Figure 1, the extension and flat springs are integrated by laser welding. The proximal end of the extension spring and the inner tube used for the surgical instrument channel are also laser-welded. The inner tube has an outer diameter of 2.5 mm and an inner diameter of 2.1 mm. It is made of stainless steel and is also integrated into the straight part of the flat spring by laser welding. The combination of the extension and flat springs can be easily bent in the distal direction of the tip, while having a relatively high stiffness in the proximal direction. This is because of the action of the lower pitch of the extension and flat springs, which are fixed by welding. This allows the DSPC to be inserted into a straight and rigid outer tube, which has a function similar to that of a conventional straight and rigid electrocautery device. In addition, when the DSPC comes out, it is restored to its original shape in a bent form, allowing it to reach narrow and deep lesions and perform electrocauterization.

When performing electrocauterization, a high stiffness in the distal direction of the tip is required. To compensate for the weak stiffness in the distal direction in the combination of the two springs, we fixed the PE line at 0.28 mm in diameter under the tip of the extension spring and improved the stiffness through tension. The reason why the stiffness can be improved by pulling the PE line is related to the pitch of the lower part of the extension spring (the opposite side to which the flat spring is in contact). When the tension is not applied, the pitch can change, thus it moves easily by external force and is inserted into the outer tube. When tension is applied to the PE line, the pitch of the lower part of the extension spring becomes zero, thus the rigidity increases. The DSPC can penetrate a variety of surgical instruments with a straight section of less than

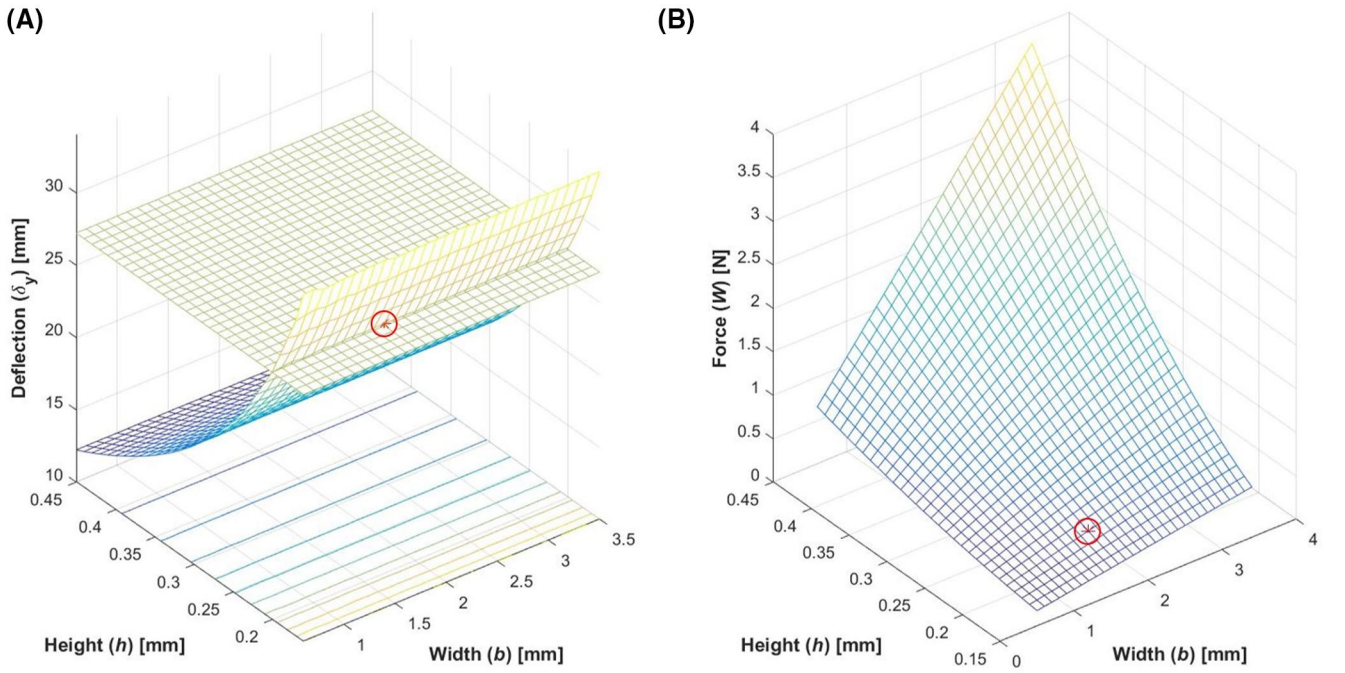

FIGURE 5 Graphs of (A) deflection and (B) force according to the height and width of the flat spring. In the deflection graph, a plane is the central axis' radius of the flat spring R_n and values above the plane are the deflection of the flat spring applicable to the DSPC $\delta_{y'}$. The circled parts show the deflection and force when $h = 0.2$ mm and $b = 1.7$ mm

1.8 mm and a curved section of less than 1.3 mm. We designed a handheld device that can move the DSPC inside a fixed outer tube made of stainless steel and could improve the stiffness by controlling the tension of the PE line. It can be controlled intuitively with 2 degrees of freedom (translation and rotation) and can easily cover a wide range of workspaces. In addition, because the DSPC can be inserted inside the rigid outer tube, it can safely reach the target position for surgical tasks.

The structure of the handheld device with the DSPC is shown in Figure 6. The device consists of a handheld part that can control the translational movement of the DSPC and a stiffness control module that can control the stiffness by changing the tension of the PE line. The size of the device is 35 mm × 60 mm × 380 mm (width × height × length), with a weight of 269 g. The DSPC is inserted into a stainless steel outer tube with an inner diameter of 3.5 mm and an outer diameter of 3.9 mm. The inner diameter was determined by considering the diameter of the PE line and the size of the circle connecting the outermost three points of the extension and flat springs, $D_O \cong 2.96$ mm, as shown in Figure 7. In the case of the DSPC translation control, a flat spring mechanism is applied similar to that in a commercially available cutter knife, and it can be easily controlled by the hand holding the device. In addition, the mechanism has the advantage that the DSPC is fixed even if a force is applied to the tip after it exits the outer tube. The PE line is wound on a roller inside the stiffness control module, as shown in Figure 6. It is easy to maintain the desired tension using a ratchet gear mechanism by turning a knob located outside.

3 | RESULTS

3.1 | Advancing accuracy and workspace

We conducted an advancing accuracy experiment for two purposes: (1) to check that the DSPC has an ideal shape when pulled out from a straight outer tube; and (2) to quantify the tip position of the drawn DSPC. The ideal shape mentioned above is the curved shape of the DSPC considering the anatomical shape of the shoulder joint shown in the previous chapter. In accordance with the DSPC control mechanism, the tip position was measured while advancing a total of 40 mm by 2.5 mm. Figure 8 shows the experimental environment. Graph paper was used as the background of the DSPC, and the position of the tip was recorded by placing a camera with a lens on top of the DSPC. The midpoint of the end of the outer tube was set as the reference point in this experiment. During this experiment, no tension was applied to the wire.

Figure 9 shows the DSPC's advancing accuracy test results. The squares and triangles represent the ideal position and the position obtained through the advancing accuracy experiment, respectively. While the DSPC advances from 2.5 to 32.5 mm, the tip position is located in the lower left corner compared to the ideal position. The average position errors in the vertical and horizontal directions were 0.78 and 0.48 mm, respectively. The remaining advance up to 40.0 mm closely matched the ideal position.

We confirmed the workspace through the trajectory when the DSPC advanced by 2.5 mm and rotated 360°. Figure 10 compares the

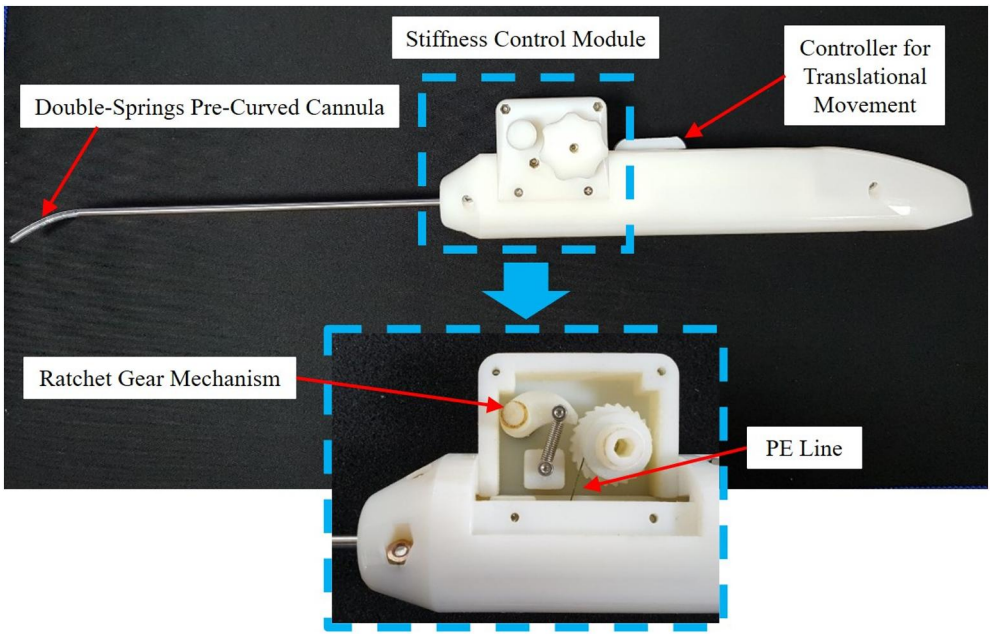

FIGURE 6 Handheld device with the double-spring pre-curved cannula and internal view of the stiffness control module consisting of a ratchet gear mechanism

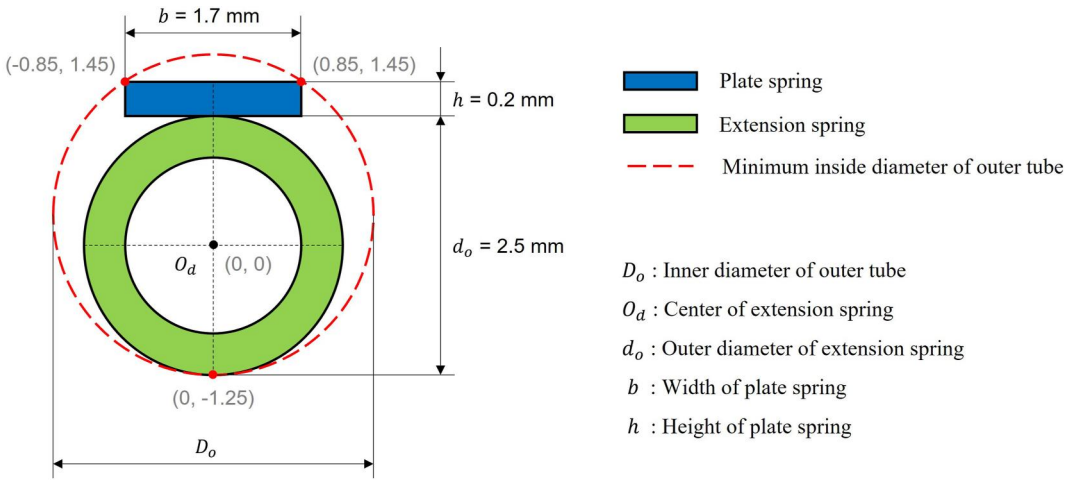

FIGURE 7 Cross section of the double-spring pre-curved cannula. A two-dimensional coordinate representation is used to calculate the inner diameter of the outer tube

workspace of the conventional straight electrocautery and the DSPC. The origin point is the position when the DSPC is completely retracted into the outer tube. The green line is the conventional device, and the red line is the DSPC advanced by 40 mm. The blue dotted lines are the tip trajectories formed when the DSPC rotates 360° while advancing by 2.5 mm.

The conventional device has a limited workspace even if it advances and rotates. In contrast, it can be seen that the DSPC has a large workspace through the advancing and rotating motions. After the DSPC advances by 2.5 mm, assuming that the entire DSPC device can advance up to 25.75 mm in the positive *z*-axis direction, it can have a workspace of 4910.63 mm^3. For example, when the DSPC advances by 17.5 mm, the *z*-axis length is 14.2 mm, and it advances from that position to 25.75 mm.

3.2 | Stiffness

We measured the stiffness against the force acting on the conventional electrocautery and the DSPC during electrocautery work. In the case of the conventional electrocautery, the stiffness acting in the direction of pressing the electrodes against the lesion was measured. In the case of the DSPC, considering the forces acting in the direction required to press the lesion and the distal direction,

we measured the stiffness acting in two directions against the scratching operation while pressing the electrode against the lesion. Figure 11 shows the experimental environment. Figure 11A is an environment in which the stiffness acting in the direction of pressing the electrodes is measured after fixing the conventional electrocautery from the portion that is 40.4 mm (the length of the DSPC) away from the tip. Figure 11B is an environment in which the stiffness acting in the upward direction is measured assuming this is when the DSPC presses a lesion. Figure 11C is an environment in which the stiffness acting in a distal direction is measured assuming that the DSPC is scratching a lesion. Figure 12 shows the upward and distal directions of the DSPC. The stiffness acting on the tip was measured using a push–pull gauge (DST-50N, IMADA), while adding up to 2 kg of weight by adding 0.2 kg to the PE line fixed to the DSPC. The push–pull gauge was fixed on a linear stage, and the force was recorded by pushing the push–pull gauge by 1 mm for each DSPC wire tension.

Table 1 shows the results of the stiffness measurement experiment of the DSPC. As the wire tension increases, it can be seen that the stiffness in both directions increases. When the wire tension was 19.6 N, the stiffnesses in the direction of the force that was pressing the lesion and the force in the distal direction were 1.38 and 1.36 N/mm, respectively. The stiffness of the conventional electrocautery was 4.60 N/mm.

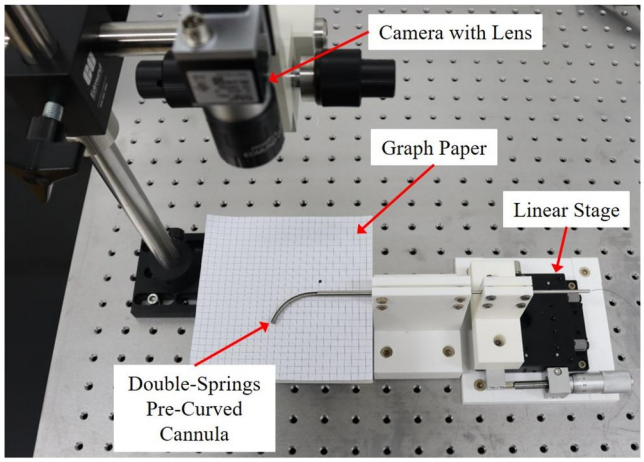

FIGURE 8 Advancing accuracy experimental environment

3.3 | Contact force and cadaveric study

We experimented with contact force measurement to obtain the force magnitude acting on the tip during electrocauterization. A measuring device was designed in a similar manner to a general electrocautery device, as shown in Figure 13. Three load cells (UU3-K50, DACELL) were mounted near the handle, allowing the force at the end to be measured in three directions. To obtain reliable data, the experiment was carried out using a cadaver with two surgeons. We measured the contact force on the skin of the cadaver, assuming that the actual patient was electrocauterized inside the shoulder joint. Two attempts were made for each surgeon, and the absolute maximum values measured for the three load cells are shown in Table 2. From the experimental data, surgeons A and B had absolute maximum forces in each direction as follows: 0.66 and 0.58 N on the *x*-axis, 1.29 and 0.71 N on the *y*-axis, and 0.86 and 1.08 N on the *z*-axis, respectively.

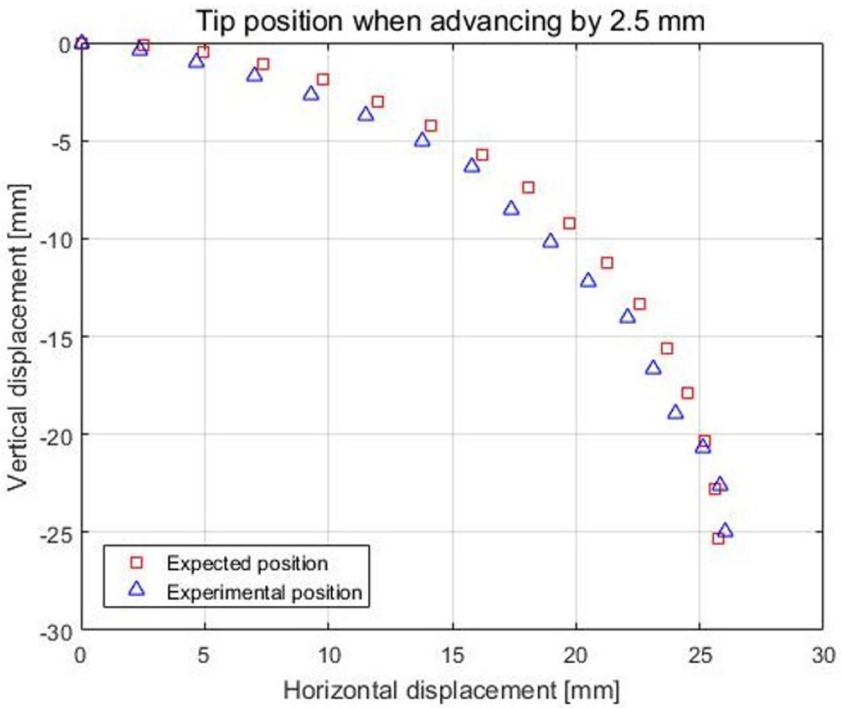

FIGURE 9 Position of the tip for each 2.5 mm advance from when the double-spring pre-curved cannula is fully retracted into the outer tube until it is fully withdrawn (40.0 mm); the squares represent the ideal position, and the triangles are the positions obtained through experimentation

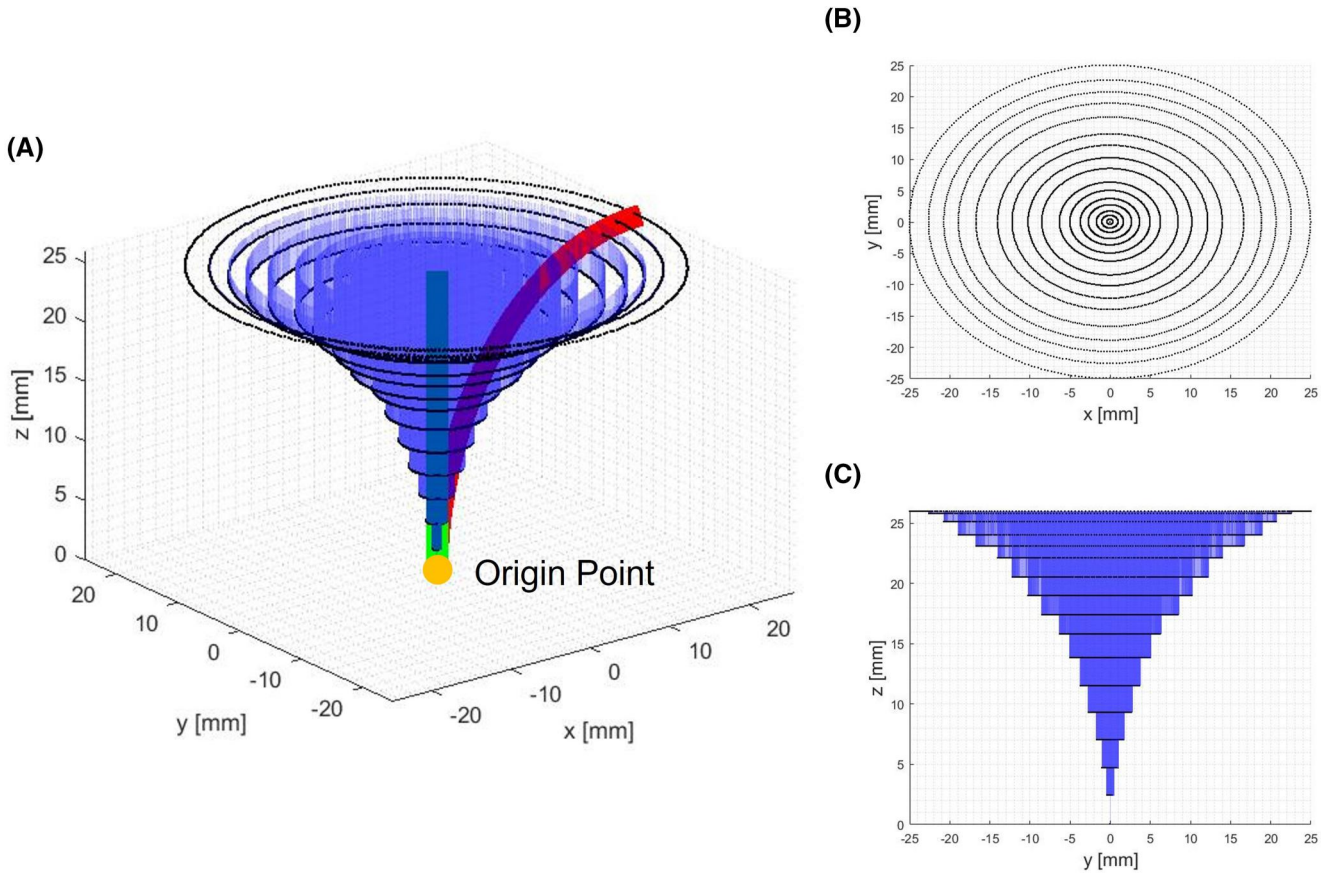

FIGURE 10 (A) Conventional electrocautery device and double-spring pre-curved cannula (DSPC) workspace comparison. The green bar is the conventional device, and the red bar is the DSPC. The black dotted lines are the trajectories of the tip formed when the DSPC rotates 360° while advancing by 2.5 mm. The blue lines are the translational trajectories that the DSPC moves to its maximum advancing depth while rotating by 1°. The yellow point is the origin point and is the position when the conventional device and DSPC do not advance. Graphs excluding the conventional device, the DSPC, and the origin point; *xy*-plane graph (B) and *yz*-plane graph (C)

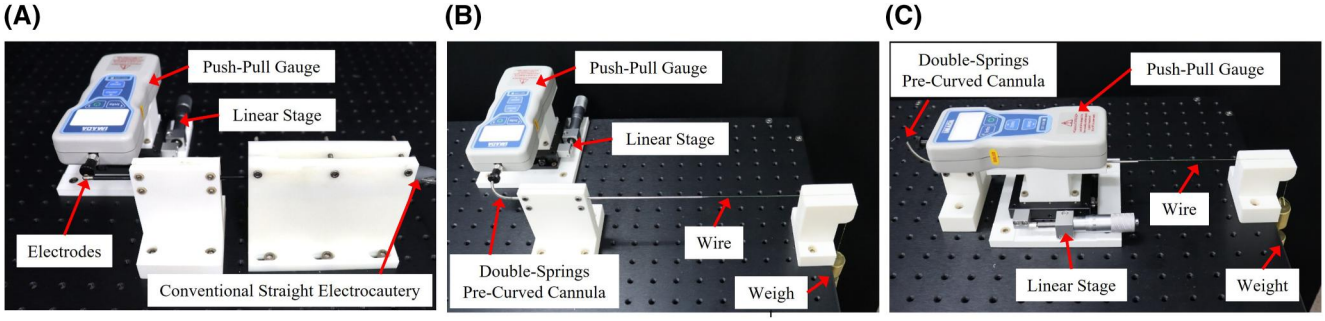

FIGURE 11 Stiffness measurement experimental environment. (A) Measuring the stiffness of the conventional straight electrocautery when it is pressing a lesion. (B) Measuring the stiffness of the DSPC when it is pressing a lesion. (C) Measuring the stiffness when the DSPC is scratching a lesion

We used a cadaver to evaluate the performance of the DSPC device inside the shoulder joint. An electrode[31] penetrated the DSPC device, and its performance was compared with that of a conventional straight and rigid electrocautery device (Super TurboVac 90, Arthrocare). We evaluated whether electrocautery work is possible in the inferior glenohumeral ligament (IGHL),[8,9,32] which is a difficult position to reach in the treatment of frozen shoulder and is located in the lower part of the glenoid inside the shoulder. Two arthroscopic images are shown in Figure 14. The conventional electrocautery had difficulty reaching the IGHL owing to the diameter of the shaft and the shape of the humeral head. In contrast, the DSPC was able to reach deep underneath the glenoid because of its small diameter and pre-curved tip.

After the cadaver study, three surgeons evaluated the performance of the device; the results are shown in Figure 15. A total of

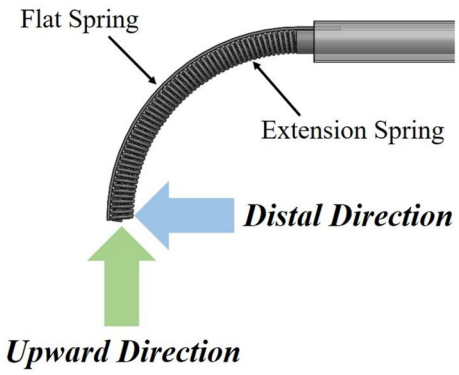

FIGURE 12 Figure showing the upward and distal directions based on the tip of the double-spring pre-curved cannula

eight items were evaluated, and each item was evaluated on a five-point scale. First, in the evaluation of the weight item, the DSPC device weighing 269 g was rated at 3.0 points, and the conventional electrocautery weighing 40 g was rated at 4.3 points. The size of the DSPC device is larger than that of the conventional electrocautery device because of the presence of the control part for translation and the wire mechanism for stiffness control. Therefore, in the evaluation of grip feeling, the DSPC device was rated at 2.0 points, and the conventional electrocautery was rated at 4.0 points. For controlling the tip and tip control interface, the DSPC device had relatively positive scores of 3.0 and 3.3 points, respectively, because it can have a large workspace with translation and rotation control. The surgeon's tiredness when manipulating the DSPC device was evaluated

TABLE 1 Double-spring pre-curved cannula's stiffness according to wire tension

Wire tension (N)	Stiffness (upward direction) (N/mm)	Stiffness (distal direction) (N/mm)
0	0.07	0.02
1.96	0.13	0.11
3.92	0.23	0.20
5.88	0.30	0.30
7.84	0.40	0.44
9.80	0.53	0.50
11.76	0.85	0.68
13.72	0.95	0.89
15.68	1.01	1.11
17.64	1.17	1.24
19.60	1.38	1.36

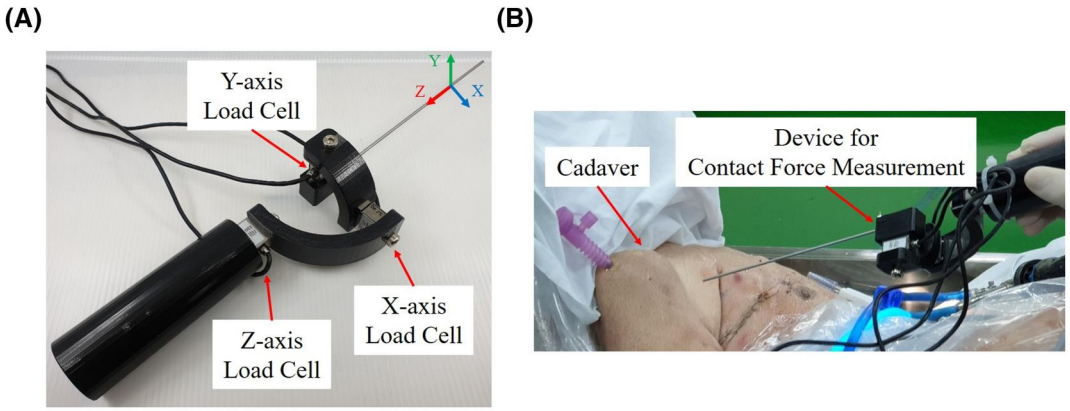

FIGURE 13 Device for contact force measurement (A) and an experiment for contact force measurement on the skin of a cadaver (B)

TABLE 2 Results of experiment for contact force measurement conducted by Surgeons A and B

	Surgeon A						Surgeon B					
	Try 1			Try 2			Try 1			Try 2		
	x	*y*	*z*	*x*	*y*	*z*	*x*	*y*	*Z*	*x*	*y*	*z*
Maximum force (N) (absolute value)	0.66	0.26	0.48	0.47	1.29	0.86	0.52	0.71	0.96	0.58	0.45	1.08

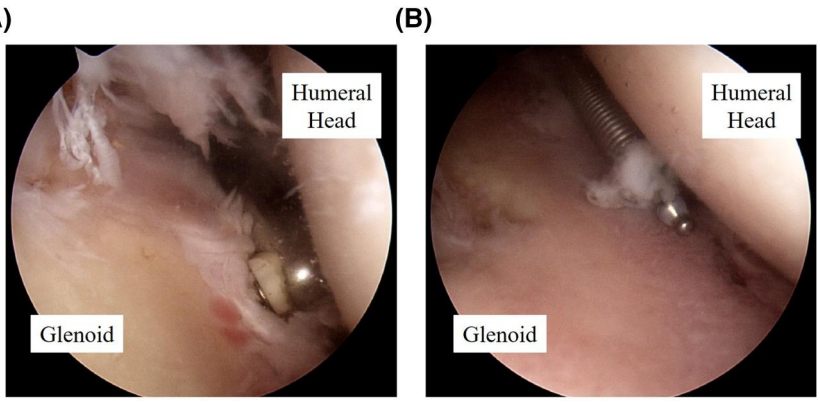

FIGURE 14 A conventional straight and rigid electrocautery device (A) and a double-spring pre-curved cannula (DSPC) device with an electrode (B) inside the shoulder of a cadaver; whereas the conventional electrocautery device had difficulty reaching the lower part of the glenoid, the DSPC device made it easily

Categories	Items
1. Appearance	1-1 Weight of the device
	1-2 Grip feeling (Size)
2. Hands-on feedbacks	2-1 Controlling the tip
	2-2 Tip control interface
	2-3 Tiredness compared to conventional design
3. End-effector	3-1 Stiffness of the tip
	3-2 Range of the tip movement
	3-3 Reach of tip in the glenoid

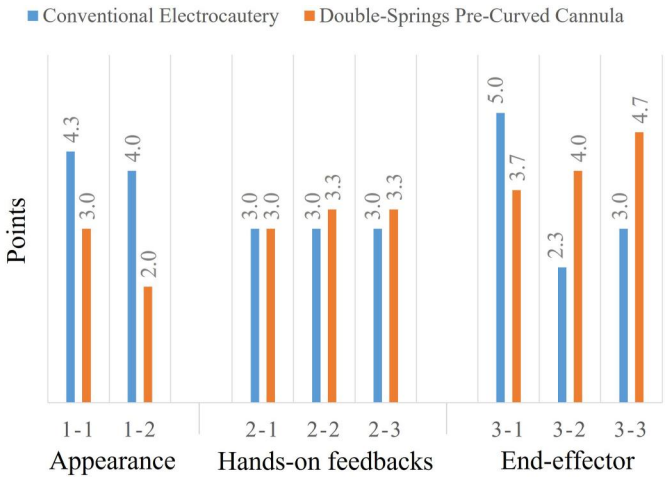

FIGURE 15 Comparison of device performance evaluation performed by three surgeons for a conventional electrocautery and the double-spring pre-curved cannula device: evaluation item table (left) and graph showing points given to each item (right)

by adjusting the wire tension to control the tip stiffness, but the evaluation demonstrated that this did not significantly affect the surgeon's tiredness (3.3 points). The tip stiffness was positively rated at 3.7 points, and the range of tip movement (4.0 points) was evaluated very positively compared to the conventional electrocautery device, which was rated at 3.2 points. In addition, the DSPC device scored 4.7 points in the evaluation of the reach of the tip in the glenoid, and this was much higher than the conventional electrocautery device, which was rated at 3.0 points. Overall, the evaluation of the two devices was similar in terms of tip control interface and tiredness, and the evaluation of the conventional electrocautery device was better in terms of weight and grip feeling. In contrast, the DSPC device had higher evaluations for tip stiffness, range of the workspace, and ability to reach the glenoid.

4 | DISCUSSION

In this study, we designed and fabricated a DSPC considering the shoulder joint's anatomy. We evaluated the tip's positional accuracy when the DSPC exited the straight outer tube at regular intervals. In addition, we confirmed that the device's stiffness increased by changing the PE line's tension in both directions. Subsequently, the surgeons verified the DSPC's performance through a cadaveric study.

Through the advancing accuracy experiment, it was confirmed that the DSPC is very close to the ideal position when it has advanced by 35.0 mm. Until then, relatively large errors occurred. There are two reasons for this: (1) the relationship between the reference point of the coordinates and the tip of the DSPC. (2) The difference between the inner diameter of the outer tube and the diameter of the DSPC. In this experiment, the reference point of the coordinates was the midpoint of the tip of the outer tube, and the position of the tip of the DSPC was the midpoint of the extension spring. Referring to Figure 7, there is an offset between the centre of the outer tube and the centre of the extension spring, and the length is approximately 0.23 mm. In addition, the difference between the inner diameter of the outer tube and the diameter of the DSPC is approximately 0.54 mm, and it is thought that an error of approximately 0.27 mm is added each time it advances because the pre-curved DSPC touches the inner wall of the outer tube. After the DSPC advances by 35.0 mm, the position error is reduced because the DSPC does not receive interference from the outer tube.

From the stiffness measurement experiment, it was confirmed that the wire tension had a great influence on the stiffness of the DSPC against the forces acting in the upward and distal directions. Although the maximum stiffness of the DSPC is smaller than that of the conventional electrocautery, by adding wire tension to the DSPC, it is possible to maintain the high stiffness required for electrocautery operations. Through the contact force measurement experiment, it was confirmed that the *y*-axis maximum stiffness value, which acts against the force in the direction in which the lesion is pressed, and the *z*-axis maximum stiffness value, which acts against the force in the distal direction, are 1.29 and 1.08 N, respectively. Because these values are smaller than those measured in the stiffness test, it is thought that there will be no problem in actual electrocautery work. Although the reliability may be somewhat degraded because the contact force measurement experiment was not conducted inside the shoulder, it was thought that the data can be referenced in this study because it is the experimental data conducted twice by two surgeons with a cadaver. To obtain more valid data in the future, we think it is necessary to attach a small sensor that can measure the force at the tip of the DSPC. In addition, regarding the stiffness of the DSPC, the stiffness changes according to the structure of the two springs and the wire tension, and this will be addressed by engineering.

An experiment comparing the performance of the two devices using the cadaver's shoulder proved that the range of the workspace and the reachability to the glenoid of the DSPC device are excellent. However, some tissues became stuck because of the space between the two springs of the DSPC and the pitch space of the extension spring. To solve this problem, we can consider covering the Teflon tube or heat shrink tube in the future. However, there could be other problems that limit the pre-curved performance of the DSPC. Therefore, in consideration of all the above-mentioned problems, it is necessary to study a sealable method that does not affect the performance of the DSPC.

The evaluation of the DSPC device performance, which was conducted by three surgeons, revealed the advantages of the device and the improvements that could be made in the future. In terms of size and weight, the DSPC device did not receive good reviews because it has various functions such as translation and stiffness control. In the future, however, the design could be modified to minimize the size while maintaining current performance, which will also reduce the weight. In addition, the wire mechanism manipulation required for stiffness control must be performed with the user's hand that is not holding the DSPC device. Therefore, if the design is modified to allow manipulation of the wire mechanism with the hand holding the device, it will be more convenient for a user to operate.

In conclusion, we developed the DSPC, which has curved movements by simple translational operation and high stiffness by wire tension, for electrocautery work. Through advancing accuracy and stiffness experiments, it was also confirmed that the DSPC has high positioning accuracy and ideal curvature as it advances from the outer tube and has a high stiffness of 1.38 N/mm compared to the diameter. Further, we demonstrated that it is possible to reach the IGHL, which is a difficult position when treating frozen shoulder, and that electric cauterization work is also possible with high stiffness. Although this study focussed on the use of the DSPC in electrocautery, and the DSPC was developed by considering only the forces acting in the distal and upward directions, we will develop it for use in forceps and curettes in the future, and we will further develop the double springs with a wire mechanism by considering the stiffness of the force acting on the side. In addition, after improving and completing the engineering quantification of the structure of the two springs and the stiffness change according to the wire tension, it will be applied as a key part of surgical robots.

ACKNOWLEDGEMENT

We thank Kitak Song, Jaeman Kwak, In-Ho Jeon (Asan Medical Center) and Chunghwan Park (Daegu-Gyeongbuk Medical Innovation Foundation) for supporting the experiments.

CONFLICT OF INTEREST

The authors declare that they have no conflict of interest.

DATA AVAILABILITY STATEMENT

The data that support the findings of this study are available from the corresponding author upon reasonable request.

ORCID

Chulmin Park https://orcid.org/0000-0002-0096-7049
Jeongryul Kim https://orcid.org/0000-0003-1893-7451

REFERENCES

1. Wiley AM. Arthroscopic shoulder surgery. *Surg Endosc*. 1987;1:65-69.
2. Ide T, Akamatsu N, Nakajima I. Arthroscopic surgery of the hip joint. *Arthroscopy*. 1991;7:204-211.
3. Cautilli R. Introduction to the basics of arthroscopy of the knee. *Clin Sports Med*. 1997;1:1-16.
4. Tingstad EM, Spindler KP. Basic arthroscopic instruments. *Operat Tech Sports Med*. 2004;12:200-203.
5. Vermesan D, Prejbeanu R. Operating setup and normal anatomy. *Atlas Knee Arthrosc*. 2015;1:1-17.
6. Kim J, Kim Y, Cho K, Kim K. Development and preclinical trials of a novel steerable cannula for 360° arthroscopic capsular release in minimally invasive surgery *Proc IEEE Eng Med Biol Soc EMBC*. 2020:4890-4894.
7. Park C, Park S, Hong H, Jeon I, Kim K. Development of an end-effector device for loose body removal in hip arthroscopy. *Proc Inst Mech Eng H*. 2018;232:1-12.
8. Pollock RG, Duralde XA, Flatow EL, Lu B. The use of arthroscopy in the treatment of resistant frozen shoulder. *Clin Orthop Relat Res*. 1994;304:30-36.
9. Burkhead WZ, Scheinberg RR, Box G. Surgical anatomy of the axillary nerve. *J Shoulder Elbow Surg*. 1992;1:31-36.
10. Resch H. Current aspects in the arthroscopic treatment of shoulder instability. *Orthopäde*. 1991;20:273-281.
11. Meyer M, Graveleau N, Hardy P, Landreau P. Anatomic risks of shoulder arthroscopy portals: anatomic cadaveric study of 12 portals. *Arthroscopy*. 2007;23:529-536.
12. Anderson PL, Lathrop RA, Webster RJ, III. Robot-like dexterity without computers and motors: a review of handheld laparoscopic instruments with wrist-like tip articulation. *Expet Rev Med Dev*. 2016;13:661-672.

13. Cepolina F, Michelini RC. Review of robotic fixtures for minimally invasive surgery. *Int J Med Robot Comp*. 2004;1:43-63.
14. Dogangil G, Davies BL, Baena FR. A review of medical robotics for minimally invasive soft tissue surgery. *Proc Inst Mech Eng H*. 2010;224:653-679.
15. Jelínek F, Arkenbout EA, Henselmans PWJ, Pessers R, Breedveld P. Classification of joints used in steerable instruments for minimally invasive surgery—a review of the state of the art. *J Med Devices*. 2015;9:010801.
16. Yoon H-S, Jeong JH, Yi B-J. Image-guided dual master-slave robotic system for maxillary sinus surgery. *IEEE Trans Robot*. 2018;34:1098-1111.
17. Kim Y, Cheng SS, Desai JP. Active stiffness tuning of a spring-based continuum robot for MRI-guided neurosurgery. *IEEE Trans Robot*. 2017;34:18-28.
18. Arata J, Saito Y, Fujimoto H. *Outer Shell Type 2 DOF Bending Manipulator Using Spring-Link Mechanism for Medical Applications*. IEEE International Conference Robotic Automation (ICRA); 2010:1041-1046.
19. Storz K, RotaTip. Accessed September 25, 2020. https://www.karlstorz.com/ru/en/s-notes.htm?countryselect=kg/2020
20. Cuschieri A. Variable curvature shape-memory spatula for laparoscopic surgery. *Surg Endosc*. 1991;5:179-181.
21. Okazawa S, Ebrahimi R, Chuang J, Salcudean SE, Rohling R. Hand-held steerable needle device. *IEEE-ASME T Mech*. 2005;10:285-296.
22. Webster RJ, III, Okamura AM, Cowan NJ. Toward active cannulas: miniature snake-like surgical robots. In *Proceedings. IEEE/RSJ International Conference Intelligent. Robots Systems (IROS)*; 2006:2857-2863.
23. Webster RJ, III, Romano JM, Cowan NJ. Mechanics of precurved-tube continuum robots. *IEEE Trans Robot*. 2009;25:67-78.
24. Kim YJ, Cheng S, Kim S, Iagnemma K. A stiffness-adjustable hyper-redundant manipulator using a variable neutral-line mechanism for minimally invasive surgery. *IEEE Trans Robot*. 2014;30:382-395.
25. Kim YJ, Cheng S, Kim S, Iagnemma K. A novel layer jamming mechanism with tunable stiffness capability for minimally invasive surgery. *IEEE Trans Robot*. 2013;29:1031-1042.
26. Cianchetti M, Ranzani T, Gerboni G, Falco ID, Laschi C, Menciassi A. STIFF-FLOP surgical manipulator: mechanical design and experimental characterization of the single module. In *Proceedings. IEEE/RSJ International Conference Intelligent. Robots Systems (IROS)*; 2013:3576-3581.
27. Cianchetti M, Ranzani T, Gerboni G, et al. Soft robotics technologies to address shortcomings in today's minimally invasive surgery: the STIFF-FLOP Approach. *Soft Robot*. 2014;1:122-131.
28. Le HM, Phan PT, Lin C, Jiajun L, Phee SJ. A temperature-dependent, variable-stiffness endoscopic robotic manipulator with active heating and cooling. *Annu Rev Biomed Eng*. 2020;48:1837-1849.
29. Jiang S, Chen B, Qi F, et al. A variable-stiffness continuum manipulators by an SMA-based sheath in minimally invasive surgery. *Int J Med Robot*. 2020;16:1-11.
30. Milner GR, Boldsen JL. Humeral and femoral head diameters in recent white American skeletons. *J Forensic Sci*. 2012;57:35-40.
31. Park CM, Kwon S, Hong H, et al. Development and preclinical trials of a wire-driven end effector device for frozen shoulder treatment. *Med Biol Eng Comput*. 2018;56:1149-1160.
32. Simmonds FA. Shoulder pain, with particular reference to the "frozen" shoulder. *J Bone Joint Surg Br*. 1949;31B:426-432.

SUPPORTING INFORMATION

Additional supporting information may be found in the online version of the article at the publisher's website.

How to cite this article: Park C, Kim J, Moon Y, Kim K. A novel arthroscopic pre-curved cannula with both flexibility and high stiffness. *Int J Med Robot*. 2022;e2360. https://doi.org/10.1002/rcs.2360